HELIUM IN AEROGEL

A minute amount of appropriately placed impurity has fascinating effects on the nature of the superfluid transitions in helium-4 and helium-3, and on the ordering of ^{3}He–^{4}He, mixtures.

Moses Chan, Norbert Mulders and John Reppy

An important theme that threads through many areas of current interest in condensed matter physics is the effect of randomness and disorder. Prior to the 1960s, disorder and impurities were often viewed as unavoidable nuisances that masked the true behavior of ideal systems. We have since learned that disorder itself can bring forth fascinating and often unexpected new phenomena in condensed phases of matter. (See the December 1988 special issue of PHYSICS TODAY, dedicated to disordered solids.)

One example is Anderson localization, in which irregularities in a metal cause localization of the wave function and render the metal insulating at low temperatures. The theoretical framework of this phenomenon, introduced by Philip Anderson some 38 years ago, has been extended to explain a host of elegant experiments on quantum transport in submicron structures and in electronic systems of reduced dimensionality.

A second example is found in glasses. Systematic studies in the 1970s and 1980s revealed that all glasses have common characteristic thermodynamic, elastic and dielectric properties that are different from those of their chemically identical, crystalline counterparts. This characteristic glassy behavior is related to the structural disorder inherent in glasses.

A third example is the Kondo effect, in which a very small quantity of magnetic impurity in a nonmagnetic metal causes a logarithmic increase in the metal's electrical resistivity with decreasing temperature, and anomalous temperature dependence in the metal's susceptibility, heat capacity and thermoelectric power.

In the statistical physics community, there is considerable interest in what are called random magnets. (See the article by Daniel Fisher, Geoffrey Grinstein and Anil Khurana in the December 1988 issue of PHYSICS TODAY, page 56.) In simple terms, random magnets are systems in which different kinds of magnetic ions or nonmagnetic ions are placed as neighbors on a lattice. Dependent on the nature of the exchange interactions between neighboring pairs of spins, and on whether there are local random magnetic fields at different sites, there are three different classes of random magnets: random exchange, random field and spin glass.

Theoretical models have been quite successful in describing the phases and phase transitions of a number of real magnetic systems. For example, a disordered Ising antiferromagnet such as $Fe_xZn_{1-x}F_2$ in a uniform magnetic field appears to be an experimental realization of the random-field Ising model. In addition to modeling magnetic systems, the random-magnet models also provide a theoretical framework for understanding collective phenomena in a number of other systems with quenched disorder. (By "quenched disorder," we mean that the positions of the impurities are fixed.) These systems and phenomena include structural phase transitions of random alloys, commensurate charge-density-wave systems with impurity pinning, melting of intercalates and "dirty" superconductors. In the case of fluids, quenched disorder can be introduced into a pure fluid system by placing the fluid in a porous medium.[1]

This article focuses on the effects of disorder on the superfluids helium-4 and helium-3, as well as on the phase separation in ^{3}He–^{4}He mixtures, that is caused by the presence of aerogel, a low-density porous material.[2] This highly porous silica glass is unique in that the quenched disorder it provides, created by a network of fibrous strands, exhibits correlations over long length scales. These long-range correlations appear to be responsible for most of the intriguing results that we describe below.

Aerogel

Aerogels were first made and given their name by Steven Kistler of Stanford University in the 1930s. They are highly porous solids, formed by a sol-gel process.[2] After the formation of the gel network, the solvent is extracted by hypercritical drying to preserve the delicate structure. The porosity is controlled by the ratio between solid and solvent used in the gelation process, and can range from 85% to as much as 99.8%. In an aerogel of 99.8% porosity, only 0.2% of the volume is occupied by silica. The density of such a sample is only four times that of air.

The initial stages of the gelation process consist of hydrolysis and polycondensation of (in our case) tetramethoxysilane. The result is the formation of small silica particles, typically 1–2 nm in diameter. Gelation is thought to be the diffusion-limited aggregation of these particles. Aggregation leads to the formation of a very open structure made up of silica strands that are connected at random sites. The interconnectivity produces a solid that is highly compressible and yet mechanically robust.

MOSES CHAN *is a professor of physics, and* NORBERT MULDERS *is a research associate, at Pennsylvania State University in University Park.* JOHN REPPY *is a professor of physics at Cornell University in Ithaca, New York.*

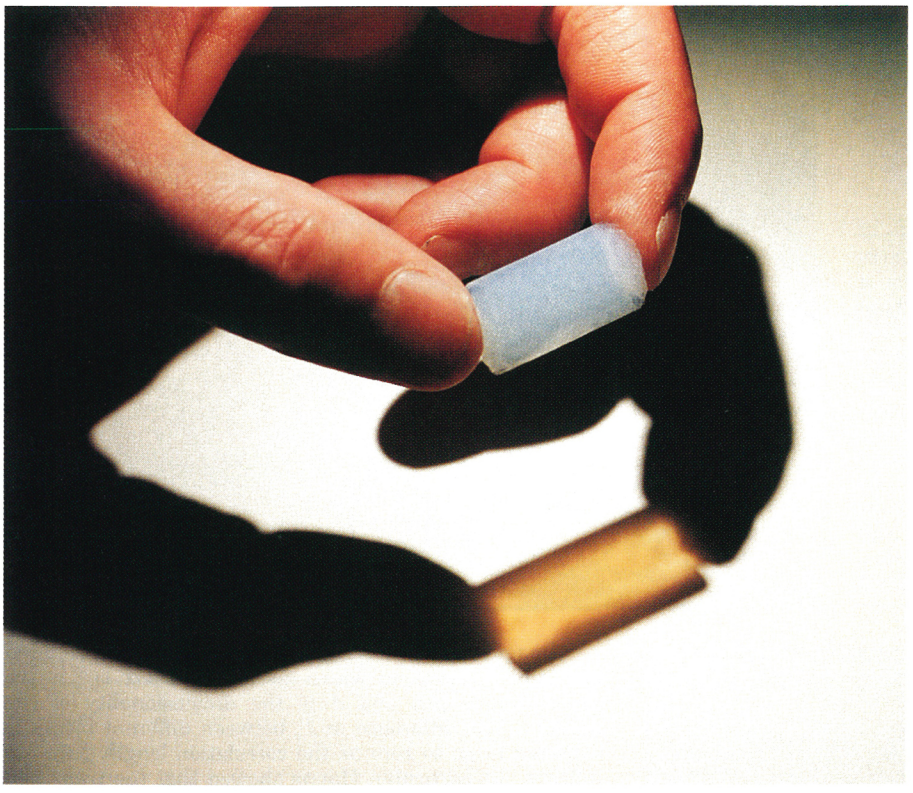

AEROGEL of 95% porosity, photographed under white light. The bluish tint of the sample and the yellowish tint of the transmitted light are consequences of Rayleigh scattering. FIGURE 1

Figure 1 is a photograph of an aerogel sample of 95% porosity. The sample is translucent. Under white light it appears bluish, while the transmitted light is yellow. This is a consequence of Rayleigh scattering, the phenomenon responsible for blue sky and red sunsets.

Figure 2 shows a representative transmission electron microscope picture, taken by George Ruben of Dartmouth College, of a 98.5% porous aerogel grown by Lawrence Hrubesh and Thomas Tillotson of Lawrence Livermore National Laboratory. The corresponding small-angle x-ray scattering (SAXS) data were gathered by Laurence Lurio and Mulders at the National Synchrotron Light Source at Brookhaven National Laboratory. The SAXS data show fractal-like correlations in the mass distribution, on length scales up to 65 nm. In lighter aerogels, this correlation is extended to longer length scales. However, SAXS data do not tell us much about the connectivity of the silica network.

Recent interest in the material has been promoted by its utilization as the refractive medium in Čerenkov detectors. Aerogel is also commercially produced as a thermal insulating material. Other applications include catalysis, catalyst support, gas storage, gas filtering and as a medium to capture interstellar particles in space missions.

Superfluid transition of ^{4}He in aerogel

The superfluid density and heat capacity of ^{4}He in a 94% porous aerogel, measured by Gane Wong while he was at Cornell University,[3] are shown in figure 3b. As in the case of pure ^{4}He (figure 3a), the superfluid density vanishes at the same temperature at which one finds a maximum in the heat capacity. (See box 1 for a definition of superfluid density and a discussion of the superfluid transition in pure ^{4}He.) This property strengthens the interpretation that the transition in the ^{4}He/aerogel system is indeed a genuine phase transition. Remarkably, in spite of the random environment, the transition remains exceedingly sharp. It is indeed one of the sharpest transitions observed. The sharpness is demonstrated more clearly in figure 4, which shows that ρ_s for helium in aerogel, as well as for pure helium and helium in Vycor, has a simple power-law dependence in the reduced temperature t. (See box 1.) (Vycor is the trade name of a porous silica glass manufactured by Corning Glassworks; its porosity is 30%. Transmission electron microscopy shows that the pore structure can be visualized as interconnected wormlike channels approximately 7 nm in diameter.) In the case of helium in aerogel, this simple power-law behavior extends down to $t = 10^{-4}$. The exponent characterizing the power law, deduced from data between $t = 10^{-4}$ and 10^{-2}, however, is found to be 0.81, significantly larger than the value for pure ^{4}He.

In pure ^{4}He the critical exponents and amplitude ratios at elevated pressures are identical to those at saturated vapor pressure if one includes pressure-dependent corrections. To investigate whether or not this universal (that is, pressure-independent) behavior applies equally in the ^{4}He/aerogel system, second-sound measurements were made at the University of California, Santa Barbara,[4] for a range of pressures up to 2.5 megapascals. Using a model for sound propagation in superfluids in a highly compliant matrix, developed by Julian Maynard at Pennsylvania State University, it was possible to determine the superfluid density from the second-sound speed. The results at saturated vapor pressure confirmed the Cornell results—that the dependence of ρ_s on t can be described by a simple power law with an exponent close to 0.8. With increasing pressure, however, the exponent becomes larger, and systematic deviations from a simple power law become more apparent. It thus becomes clear that, as in the case of pure ^{4}He, pressure-dependent corrections to scaling terms have to be included in the analysis of the data. When correction is done, a universal exponent, ζ, is recovered. This exponent remains signifi-

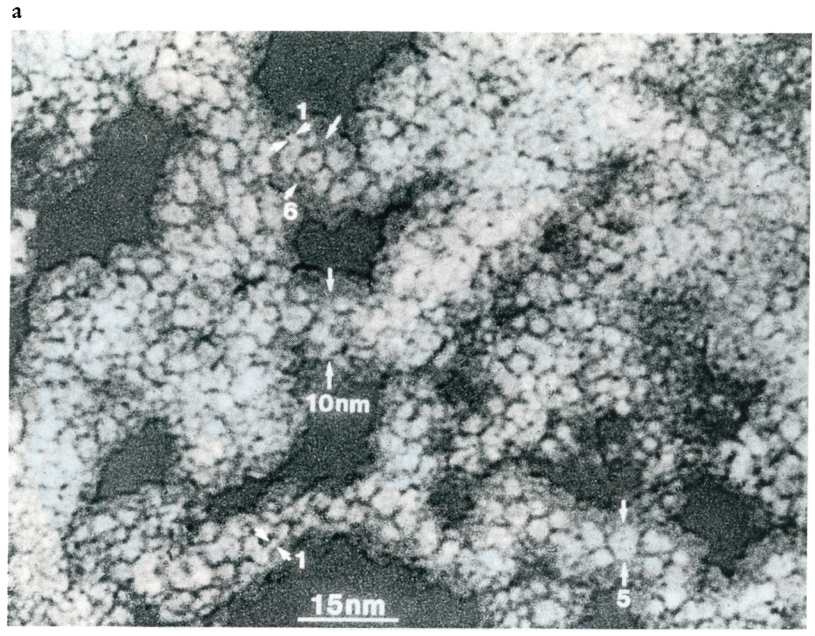

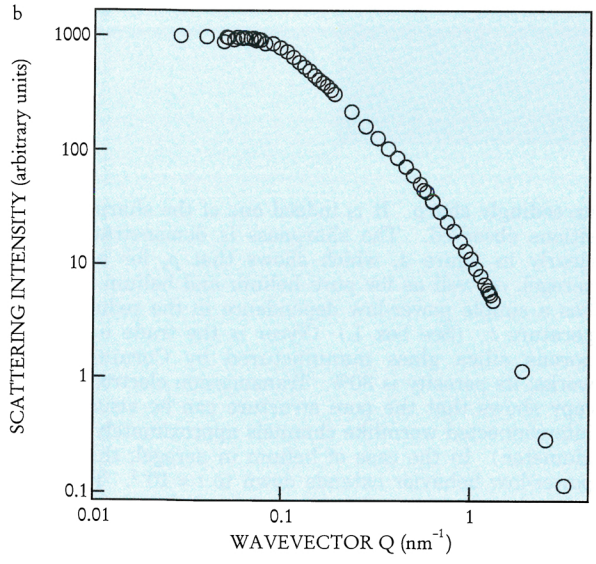

TRANSMISSION ELECTRON MICROGRAPH (a) and a plot of small-angle x-ray scattering data (b) of an aerogel of 98.5% porosity. The micrograph shows that silica nodules of about 1 nm connect and form a random fibrous network. The numbers indicate approximate distances in nanometers. Scattering at a wavevector Q originates from density–density correlations at a length scale of $2\pi/Q$. The data show fractal-like correlations in the mass distribution in the sample up to a length scale of 65 nm. FIGURE 2

cantly larger than that for pure ^{4}He: $\zeta_{aero} = 0.75$ versus $\zeta_{pure} = 0.67$. Experiments at Cornell and Santa Barbara on aerogels of lower porosity—for example, of 91% porosity—found ζ_{aero} similar to that for 94% aerogel.

The effect of quenched disorder on the superfluid transition can be treated as analogous to random exchange in a magnetic system. Nonmagnetic impurities in an otherwise pure magnetic sample lead to spatial inhomogeneities in the locally averaged strength of the magnetic interaction. Because the transition temperature depends on the strength of this averaged interaction, the effect of impurities can be modeled as a distribution of locally defined transition temperatures, $T_c(r)$. At first glance, one might expect that this effect would lead to a rounded or smeared transition. In 1974, A. Brooks Harris of the University of Pennsylvania showed that such a result is not necessarily the case, provided there is no long-range correlation in the positions of the impurities. This argument was later confirmed by more rigorous renormalization-group calculations.[5]

Imagine that the sample is divided into uncorrelated blocks of ξ^d spins, in which (as noted in box 1) ξ is the correlation length and d is the dimensionality of the system. The difference in T_c between different blocks is expected to go to zero as the correlation length grows to infinity. In particular, Harris showed that the transition will be stable against the smearing effect of the disorder if the fluctuations in the local $T_c(r)$ go to zero faster than $|T - T_c|$ as $\xi \to \infty$. This stability criterion, named after Harris, can be written in terms of the critical exponents for the pure system:

$$2 - d\nu_{pure} = \alpha_{pure} < 0$$

Accordingly, a pure system that satisfies the Harris criterion would, after impurity dilution, still undergo a sharp phase transition with the same critical exponents as the pure system. Because $\alpha = -0.013$ for the superfluid transition of pure ^{4}He, one would expect the Harris criterion to be satisfied for ^{4}He in porous media. In fact, superfluid density measurements of ^{4}He in porous Vycor glass found a sharp transition,[1,3] as is shown in figure 4, with a critical exponent, ζ, that matches that of bulk ^{4}He. This agreement is all the more remarkable if one remembers that in Vycor glass, silica constitutes 70% of the volume. This agreement also leaves the result of ^{4}He in aerogel even more intriguing.

There is as yet no quantitative understanding of the difference in the critical behavior in these two systems. However, it is most likely related to the pore structure. As noted above, transmission electron microscope pictures of Vycor show an interconnected network of pores with a well-defined diameter. This network configuration is confirmed by small-angle neutron scattering measurements, which reveal a dominant length scale of 27 nm. Thus, there is no correlation in the position of the silica over length scales longer than 27 nm. In contrast, there is no such characteristic length scale in aerogel. Fractal-like correlations appear to extend up to approximately 100 nm. Beyond 100 nm, SAXS data imply a uniform structure (see figure 2). Assuming the Josephson relation (see box 1) to be applicable in the aerogel system, the correlation length is approximately 120 nm at $t = 10^{-3}$ and 600 nm at $t = 10^{-4}$. It is therefore surprising that for $t < 10^{-3}$ the critical behavior is still different from that of pure ^{4}He. It was noted by Onuttom Narayan of the University of

Box 1. The superfluid transition in ^{4}He

Owing to its small mass and correspondingly large zero-point motion, as well as the very weak attraction between the highly symmetric atoms, helium remains liquid down to absolute zero. To produce the solid phase requires a pressure of 2.5 megapascals. At low temperature, the liquid displays one of the most striking of macroscopic quantum phenomena—namely, superfluidity. (See also John Bardeen's article in the December 1990 issue of PHYSICS TODAY, page 25, for a discussion of macroscopic quantum phenomena, and Russell Donnelly's article in the July 1995 issue, page 30, for an account of the discovery of superfluidity.) In ^{4}He the phase transition between the normal and superfluid phases takes place at a somewhat pressure-dependent temperature T_c of about 2.17 K, below which the liquid shows the astonishing ability to flow without friction through narrow channels.

Many aspects of superfluid behavior can be understood within the context of the two-fluid model, first suggested by Laszlo Tisza in 1938. This model assumes that the superfluid consists of two completely interpenetrating components—a normal fluid with properties very similar to those of any ordinary fluid, and a superfluid that carries no entropy and has no viscosity. The total density of the liquid is the sum of the superfluid and normal fluid densities: $\rho = \rho_s + \rho_n$. A convenient parameter in the description of this system is the superfluid fraction ρ_s/ρ, which grows from zero at T_c to one at $T = 0$.

The superfluid density can be conveniently determined in two ways. In 1946, Elevter Andronikashvili used a torsional pendulum to determine ρ_s in bulk ^{4}He. Suspended from a torsional fiber, a cylindrical stack of disks, sufficiently closely spaced to viscously drag the normal fluid, was immersed in liquid helium. When the helium was cooled below the transition, the superfluid part of the liquid decoupled from the motion of the pendulum, causing a change in its resonance frequency. This technique has been improved upon considerably, mainly by replacing the fiber with a stiff, hollow torsion rod. This torsion rod, typically on the order of 1 mm in diameter and 1 cm in length, is normally made of a beryllium–copper alloy. It is attached to a thin-walled cell that contains a porous substrate, and that also allows helium to be introduced into the cell. The cell and torsion rod form a pendulum, which is electrostatically driven at its torsional mode. The resonance frequency will depend on the ratio of the stiffness of the torsion rod and the total moment of inertia of the cell. Above the superfluid transition the helium is viscously locked to the substrate and contributes its entire moment of inertia, usually less than 1% of the total, to the pendulum bob. However, when the temperature is lowered below T_c, this contribution is reduced, because the superfluid partially decouples from the substrate. This decoupling from the motion of the oscillator results in a shift in resonance frequency proportional to the superfluid density. The torsional oscillator technique is particularly suitable for the detection of superfluidity in porous media.

One of the predictions of the two-fluid model is that, in addition to a normal pressure-density sound mode, the superfluid also supports a propagating temperature/entropy mode. The velocity of this mode, which has become known as second sound, is primarily a function of the superfluid density. Thus second-sound measurements are an alternative, and often preferred, method to determine ρ_s. The two-fluid model can be extended straightforwardly to take into account the viscous coupling between a porous medium and the normal fluid. Thus, acoustic measurements can also be used to obtain the superfluid density in porous media.

The superfluid transition in ^{4}He, also called the λ-transition because of the characteristic shape of the accompanying heat capacity peak (figure 3a), provides the most convincing experimental confirmation of the scaling and renormalization group theory of critical phenomena.[17] Such an assessment is based on the excellent agreement between the measured and predicted heat capacity, C, and superfluid density, ρ_s, in the vicinity of the transition. According to modern theory of critical phenomena, very close to the transition, ρ_s and C are expected to exhibit power-law dependence on the reduced temperature $t = |T - T_c|/T_c$, of the form

$$\rho_s(t) = \rho_{s0}\, t^{\zeta} \qquad \text{for } T < T_c \tag{1}$$

$$\rho_s(t) = 0 \qquad \text{for } T > T_c$$

and

$$C(t) = A/\alpha\, t^{-\alpha} \qquad \text{for } T > T_c \tag{2}$$

$$C(t) = A'/\alpha'\, t^{-\alpha'} \qquad \text{for } T < T_c \tag{3}$$

The parameters ζ and α are called critical exponents; ρ_{s0} and A are the critical amplitudes. The superfluid density is related to the correlation length, ξ, through the Josephson relation

$$\xi(t) = \xi_0 t^{-\nu} = m^2 kT/\hbar^2 \rho_s(t) \tag{4}$$

where m is the mass of the ^{4}He atom and k is the Boltzmann constant. This relationship implies that ν, the critical exponent characterizing the divergence of the correlation length, is equal to ζ. Critical exponents are universal in the sense that they depend only on the spatial dimension, d, of the system and the number of degrees of freedom of the order parameter n that characterizes the symmetry of the system. In particular, the superfluid transition in ^{4}He is thought to belong to the universality class of $d = 3$ and $n = 2$, the three-dimensional xy model. The most recent experimental values for the exponents are $\zeta = 0.6705 \pm 0.0006$ and $\alpha = -0.01285 \pm 0.00038$. These are in excellent agreement with the most reliable theoretical values[18] of 0.672 ± 0.002 and -0.016 ± 0.006.

California, Santa Cruz, and Daniel Fisher of Harvard University that because α is so close to zero, the superfluid transition satisfies the Harris criterion only marginally and the recovery to bulklike behavior is logarithmically slow.[6] Another possible explanation is that small-angle scattering data, which measure only two-point correlations, do not capture long-length-scale correlations in the connectivity of the gel network.[7]

Even more surprising are the results of the heat capacity measurements. As can be seen in figure 3, the heat capacity peak at the superfluid transition in aerogel differs dramatically from the one in pure ^{4}He. Whereas the ^{4}He one is essentially symmetrical, with identical exponents and similar amplitudes above and below the transition, this symmetry is absent in aerogel. On the high-temperature side, one still observes a significant singular contribution, whereas on the low-temperature side, one finds a linear dependence on temperature. Thermal expansion coefficient measurements (thermodynamically equivalent to heat capacity measurements) show once again that this behavior persists at elevated pressures.[8]

Given that an aerogel in which silica occupies 6% of the volume has a dramatic effect on the superfluid's critical behavior, an interesting question is how this evolves to-

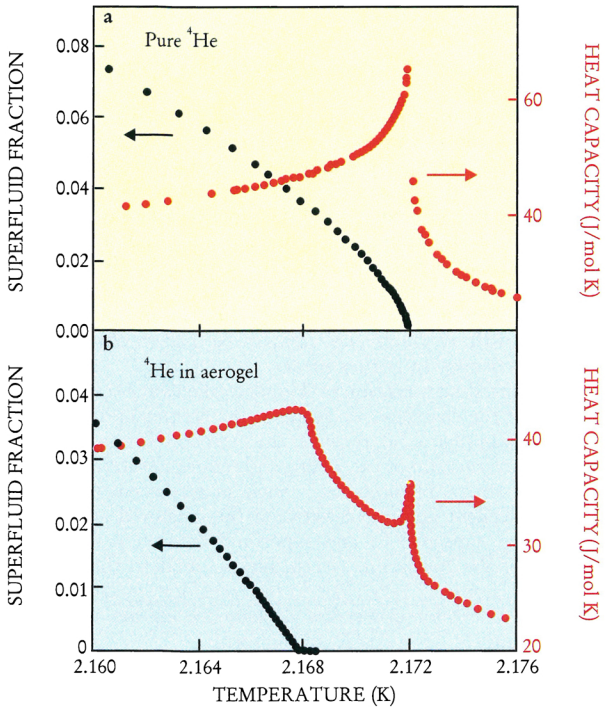

PHASE TRANSITION. Plotted are the superfluid fraction ρ_s/ρ (black) and heat capacity (red) of ^{4}He near the superfluid transition of pure ^{4}He (**a**) and of ^{4}He in aerogel of 94% porosity (**b**). In both systems the superfluid fraction vanishes at the temperature at which one finds a maximum in the heat capacity. This suggests that, in the ^{4}He/aerogel system, we are observing a genuine phase transition. The heat capacity peak in the ^{4}He/aerogel system at 2.172 K is due to helium in large voids inside the aerogel. The shape of the heat capacity peak in pure ^{4}He has lead to the name "λ-transition." FIGURE 3

ward bulk behavior when the aerogel density is further reduced. Torsional oscillator measurements on ^{4}He in aerogel that is 98% porous, made at Penn State by Jian Ma (currently at Amherst College), find a well-defined superfluid density exponent $\zeta = 0.80$ (figure 4), not very different from that found for 94% aerogel.

^{3}He–^{4}He mixtures in aerogel

Torsional oscillator experiments on ^{3}He–^{4}He mixtures in 98% aerogel produce a striking result.[9] They indicate that in this system the superfluid transition line in the phase diagram, instead of terminating at the tricritical point near 0.87 K, extends down to absolute zero. (See box 2 for a discussion of bulk ^{3}He–^{4}He mixtures, "bulk" meaning without aerogel.) As figure 5 shows, the coexistence region is completely contained within the superfluid part of the phase diagram. Phase separation is now a transition between the usual ^{4}He-rich superfluid and a new ^{3}He-rich superfluid. The tricritical point is replaced by a regular critical point at the top of the coexistence curve.

This phase diagram is deduced from the following experimental observations. The frequency and amplitude of the torsional oscillator, which is operated at constant drive, are monitored as a function of temperature. After a temperature scan at a particular ^{3}He concentration is completed, the concentration is changed and the next temperature scan is made. The superfluid transition in such a scan is marked by the decoupling of the superfluid from the motion of the oscillator. At high ^{3}He concentration, this decoupling is the only feature that is detected. "High concentration" means that the ratio $N_3/(N_3+N_4)$ is greater than 0.8, where N_3 and N_4 are the numbers, respectively, of ^{3}He and ^{4}He atoms in the mixture. At lower ^{3}He concentration, one finds at a temperature below the superfluid transition a second feature—namely, a sharp dip in the amplitude of the oscillator. This dip is taken as the signature of the miscible mixture phase separation into ^{3}He-rich and ^{4}He-rich phases. This interpretation is reinforced by the observation of hysteresis in the oscillator frequency inside the coexistence region.

An interesting question is how the system organizes itself to be able to support superfluidity at high ^{3}He concentrations, whereas this is normally not possible in mixtures without the aerogel (see box 2). Because ^{4}He has a smaller zero-point motion than ^{3}He, it can profit more from the attractive van der Waals interaction between helium and silica. At high ^{3}He concentration and a temperature far below the ^{3}He–^{4}He critical point, the ^{4}He atoms are plated out of the mixture onto the silica strands and form a solidlike layer, similar to that found in experiments of adsorbed ^{4}He films. After completion of the localized solid layer, the ^{4}He atoms are still expected to accumulate near the silica strands, instead of being homogeneously distributed among the ^{3}He. At low temperatures, where the solubility of ^{4}He in ^{3}He is low, this process should lead to the formation of a well-defined ^{4}He-rich film. The superfluid transition can now be thought of as taking place purely in this film.[10]

The main argument against this picture for mixtures in aerogel comes from heat capacity measurements. A recent experiment used torsional oscillator and heat capacity techniques to study superfluid transitions of ^{4}He films adsorbed from vapor onto the silica strands in aerogel.[11] It was found that, based on the disappearence of the superfluid density, the transition is quite sharp, but not accompanied by any measurable peak in the heat capacity. With the mixtures in aerogel, the situation is quite different.[9] At low ^{3}He concentrations, one finds a heat capacity peak at the superfluid transition, very similiar to that in bulk mixtures. But whereas in bulk this peak decreases in size with increasing ^{3}He concentration and vanishes at the tricritical point, in aerogel it persists and can be observed all along the superfluid transition line. Indeed, the phase diagram for mixtures in 98% aerogel based on heat capacity results is consistent with that shown in figure 5.

Recent density functional calculations and path integral Monte Carlo simulations of bulk mixtures found[12] that the size of the ^{3}He–^{4}He interface is on the order of 1 nm. Such a diffuse interface increases substantially the effective thickness of the ^{4}He film and thus enhances the three-dimensional connectivity established by the aerogel. This mechanism is most likely responsible for the three-dimensional–like superfluidity observed at low tempera-

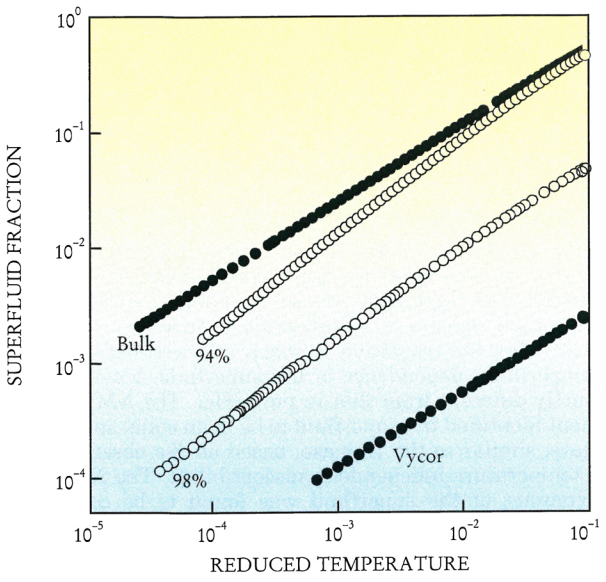

SUPERFLUID FRACTION ρ_s/ρ as a function of the reduced temperature $t = (T_c - T)/T_c$, for pure ^{4}He, for ^{4}He in Vycor and for ^{4}He in aerogels of 94% and 98% porosity. For the sake of clarity, the value of ρ_s/ρ for the 98% aerogel has been multiplied by 0.1 and for ^{4}He in Vycor by 0.01. The Vycor data are parallel to those of pure ^{4}He, implying identical superfluid density exponents. The exponent for ^{4}He in aerogel is clearly larger. FIGURE 4

tures. In such a scenario, the coexistence region at low temperatures is likely to correspond to "capillary condensation" of the ^{4}He film from neighboring silica strands into ^{4}He-rich domains. With increasing ^{4}He concentration, increasingly larger pockets are formed. On the ^{4}He-rich side of the phase diagram, coexistence ends when the last ^{3}He-rich domain, presumably situated farthest from any silica strand, shrinks out of existence. With increasing temperature, ^{4}He atoms will progressively "evaporate" into the ^{3}He-rich domains, giving rise to a more homogeneous solution. The ^{3}He–^{4}He critical point marks the maximum temperature where ^{3}He- and ^{4}He-rich domains are found.

These results have stimulated a number of recent theoretical studies. Amos Maritan and his collaborators at the University of Padua, in Italy, and at Penn State take the silica strands as a source of quenched randomness that favors ^{4}He atoms.[13] Within the Blume–Emery–Griffiths model, the tricritical point was found to be unstable, which can lead to a phase diagram that resembles the one shown in figure 5. By constructing a correlated random chemical potential model to mimic the connectivity of the aerogel, Alexis Falicov and Nihat Berker of MIT obtained a mixture phase diagram remarkably similar to what is deduced from experiment (figure 5).[14]

Interestingly, the new superfluid phase at high ^{3}He concentrations appears even in aerogels of much lower density. This is illustrated in figure 6, which shows a comparison between the heat capacity of bulk mixtures and that for mixtures in 99.5% aerogel, on the ^{3}He-rich side of the phase diagram. The discontinuity associated with the phase separation in the bulk, although somewhat broadened, is still clearly visible in the aerogel. In addi-

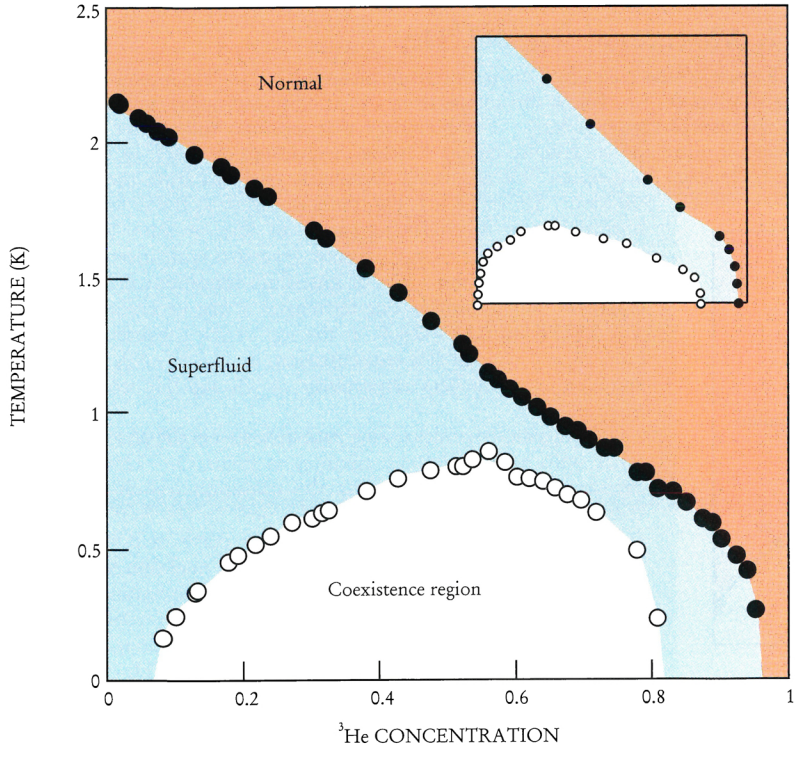

MEASURED AND CALCULATED (inset) phase diagrams of ^{3}He–^{4}He mixtures in aerogel of 98% porosity. In contrast to what one observes in bulk mixtures (that is, without aerogel), there is no tricritical point. (See box 2.) The transition line between the normal (red) and superfluid (blue) phases is detached from the coexistence curve, and the coexistence region resides entirely within the superfluid part of the phase diagram. The top of the coexistence curve now corresponds to a regular critical point. Alexis Falicov and Nihat Berker of MIT did the calculation. FIGURE 5

tion, there is a peak at higher temperature related to the superfluid transition, which is conspicuously absent in the bulk mixtures.

Superfluid transition of ^{3}He in aerogel

Having seen these remarkable new phenomena associated with the introduction of aerogel into both liquid ^{4}He and ^{3}He–^{4}He mixtures, one can ask what the consequences might be in the case of the ^{3}He/aerogel system. It is known that ^{3}He is the paradigm of exotically paired superfluids, in which the Cooper pairs exhibit a pairing other than the usual s-wave symmetry of ordinary superconductors. The ^{3}He undergoes a superfluid transition at temperatures between 2.5 mK (at high pressure) and 0.9 mK (at vapor pressure). In the bulk, the A phase (with spin pairing $|\uparrow\uparrow\rangle + |\downarrow\downarrow\rangle$) is favored over the B phase ($|\uparrow\uparrow\rangle + |\downarrow\downarrow\rangle + |\downarrow\uparrow + \uparrow\downarrow\rangle$) only at high pressure and close to the transition temperature. The pairing length is on the order of several tens of nanometers. Because diffuse quasiparticle scattering at boundaries breaks Cooper pairs and suppresses the superfluidity over a length scale on the order of a coherence length, confinement of the superfluid within the pore structure of conventional porous materials having micrometer-sized pores can reduce T_c appreciably. Confinement in pores with diameters less than a few tens of nanometers destroys the superfluidity altogether.

In the ^{3}He/aerogel system, every point in the fluid is less than a coherence length away from a silica strand. Nevertheless, recent torsional oscillator and nuclear magnetic resonance (NMR) experiments at Cornell University[15] and Northwestern University[16] found that in 98% aerogel, the superfluid phase is stable. Although the superfluid density is significantly reduced (compared to pure ^{3}He), the transition is sharp and well defined. The temperature dependence of the superfluid density is distinctly different from that in pure ^{3}He. The NMR experiment identified the superfluid to be in an equal spin-paired state, similar to the A phase, based on the observation of a temperature-independent susceptibility. The NMR spin dynamics of the superfluid was found to be completely altered inside the aerogel.

The fact that the superfluid phase is stable in aerogel is probably related to the fact that quasiparticle scattering by aerogel is qualitatively different from what happens in more conventional porous media. The size of the gel strands is on the order of 5 nm, much less than the superfluid coherence length, and the mean free path for the ^{3}He quasiparticles within the aerogel is significantly longer than the mean distance between strands. Thus it seems that the scattering of the quasiparticles by the aerogel is more appropriately described by impurity scattering than by scattering from solid boundaries.

Some key aspects of this problem are being addressed in ongoing theoretical work at Northwestern University, Helsinki University of Technology and the Landau Institute of Theoretical Physics in Moscow. Attempts to model the aerogel as an isotropic scattering medium, however, found that the B phase is more stable than the A phase,

Box 2. Mixtures of ^{3}He and ^{4}He

The accompanying figure shows the phase diagram in the concentration/temperature plane for a ^{3}He–^{4}He mixture. Above 0.872 K, liquid ^{3}He and ^{4}He are miscible in all proportions. Below this temperature a miscibility gap opens up in the phase diagram; this gap is conventionally called the coexistence region (white). The boundary that separates this region from the miscible superfluid (blue) and normal (red) phases is called the coexistence curve. Owing to quantum statistics, in the $T = 0$ limit the ^{4}He-rich fluid can still contain up to 6.4% ^{3}He. In contrast, ^{4}He atoms are completely excluded from the ^{3}He-rich solution. Above 0.872 K the transition between the superfluid and normal phases is similar in nature to that in pure ^{4}He. The superfluid transition temperature is depressed with increasing ^{3}He concentration, tracing a line of superfluid transitions in the phase diagram. This transition line terminates at the tricritical point at $T = 0.872$ K and $X_3 = 0.669$, at the top of the coexistence curve. Here X_3 is the molar ^{3}He concentration, or $N_3/(N_3+N_4)$, where N_3 and N_4 are the numbers, respectively, of ^{3}He and ^{4}He atoms in the mixture.

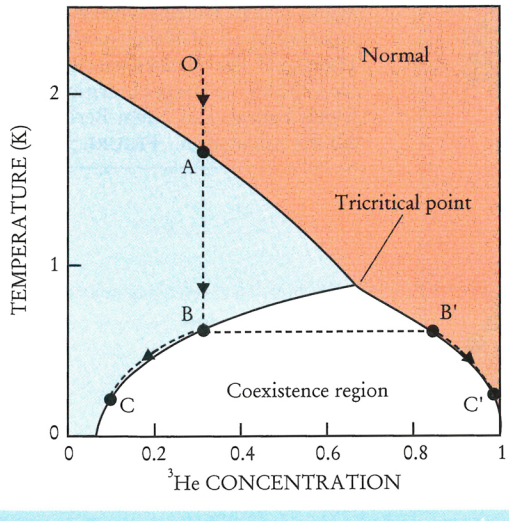

The thermodynamic cooling path indicated in the phase diagram starts with a normal fluid mixture, at point O. This mixture becomes superfluid on crossing the transition line at A. The transition is accompanied by a λ-like peak in the heat capacity. Subsequently, on meeting the coexistence curve at point B, the mixture phase separates, and a ^{3}He-rich phase nucleates with X_3 as defined by B′. Here, the heat capacity shows a discontinuity. On further reduction of the temperature, the ^{3}He concentrations of the two phases are specified by the coexistence curve—along the paths B → C and B′ → C′. Starting with a mixture with a ^{3}He concentration of $X_3 > 0.669$, the superfluid transition is absent and only phase separation is observed. (See figure 6b.)

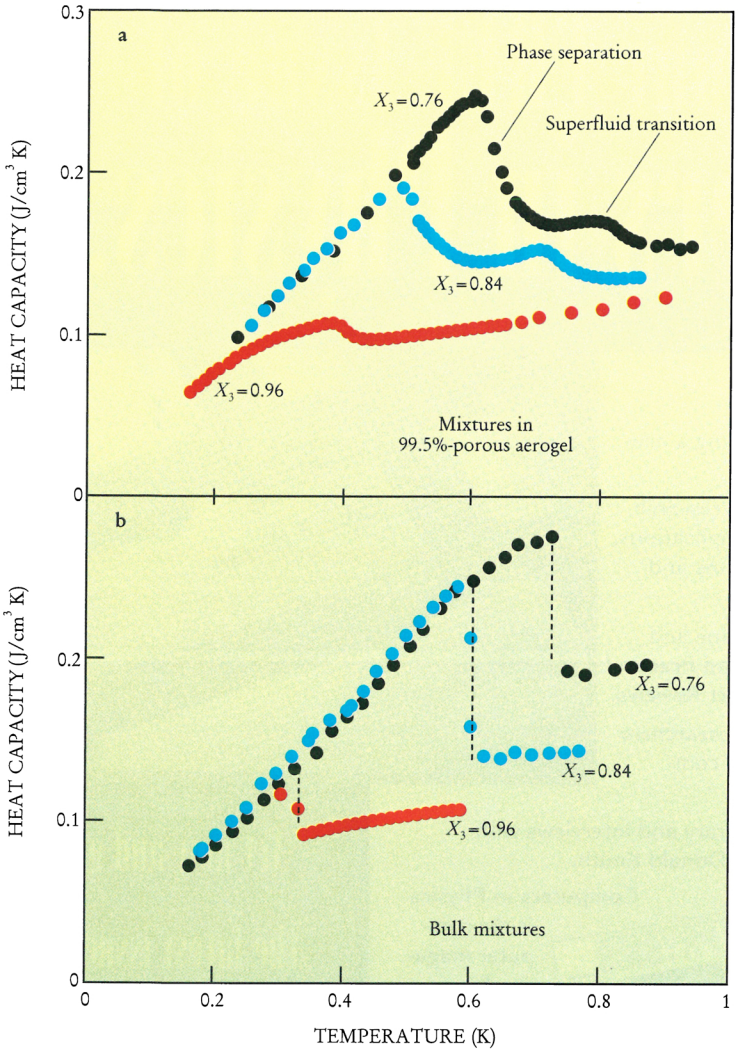

HEAT CAPACITY of ^{3}He-rich ^{3}He–^{4}He mixtures in aerogel of 99.5% porosity (**a**), and without aerogel (**b**). The discontinuity observed in the bulk corresponds to phase separation. Inside the aerogel, this signature is broadened. In addition, one finds a peak in the heat capacity associated with the superfluid transition, which at these concentrations is absent in the bulk. The parameter X_3 is the molar ^{3}He concentration.
FIGURE 6

in contrast to what is found experimentally. Anisotropic scattering induced by the geometry of the strand may lead to stabilization of the A phase, but as yet the details of both NMR and torsional oscillator experiments have not been explained by the theoretical models. Nevertheless, the existence of a stable ^{3}He superfluid phase in aerogel, and the extension of the superfluid transition line to $T = 0$ as shown in figure 5, opens the possibility of finding a system of two interpenetrating superfluids.

We thank Lawrence Hrubesh for introducing us to the fine art of aerogel making. We gratefully acknowledge support provided by the National Science Foundation.

References

1. For a recent review of the superfluid transition of ^{4}He in porous media, see J. D. Reppy, J. Low Temp. Phys. **87**, 205 (1992).
2. For the most recent results on aerogel, see R. W. Pekala, L. W. Hrubesh, eds., *Proceedings of the Fourth International Symposium on Aerogel*, North Holland, Amsterdam (1995) [J. Non-Cryst. Solids, **186** (1995)]. For a more informal account, see J. Fricke, Sci. Am., May 1989, p. 92.
3. M. H. W. Chan, K. I. Blum, S. Q. Murphy, G. K.-S. Wong, J. D. Reppy, Phys. Rev. Lett. **61**, 1950 (1988). G. K.-S. Wong, P. A. Crowell, H. A. Cho, J. D. Reppy, Phys. Rev. B **48**, 3858 (1993).
4. N. Mulders, R. Mehrotra, L. S. Goldner, G. Ahlers, Phys. Rev. Lett. **67**, 695 (1991).
5. A. B. Harris, J. Phys. C **7**, 1671 (1974). J. T. Chayes, L. Chayes, D. S. Fisher, T. Spencer, Phys. Rev. Lett. **57**, 2999 (1986).
6. O. Narayan, D. S. Fisher, Phys. Rev. B **42**, 7869 (1990). For further references on current theories about the superfluid transition in aerogel, see K. Moon, S. M. Girvin, Phys. Rev. Lett. **75**, 1328 (1995).
7. D. W. Schaefer, C. J. Brinker, D. Richter, B. Fargo, B. Frick, Phys. Rev. Lett. **64**, 2316 (1990).
8. M. Larson, N. Mulders, G. Ahlers, Phys. Rev. Lett. **68**, 3896 (1992).
9. S. B. Kim, J. Ma, M. H. W. Chan, Phys. Rev. Lett. **71**, 2268 (1993). N. Mulders, M. H. W. Chan, Phys. Rev. Lett. **75**, 3705 (1995).
10. J. P. Romagnan, J. P. Laheurte, J. C. Noiray, W. F. Saam, J. Low Temp. Phys. **70**, 425 (1978).
11. P. A. Crowell, J. D. Reppy, S. Mukherjee, J. Ma, M. H. W. Chan, D. W. Schaefer, Phys. Rev. B **51**, 12712 (1995).
12. L. Pricaupenko, J. Treiner, Phys. Rev. Lett. **74**, 430 (1995). M. Bonisegni, D. M. Ceperley, Phys. Rev. Lett. **74**, 2288 (1995).
13. A. Maritan, M. Cieplak, M. Swift, F. Toigo, J. R. Banavar, Phys. Rev. Lett. **69**, 221 (1992).
14. A. Falicov, A. N. Berker, Phys. Rev. Lett. **74**, 426 (1995).
15. J. V. Porto, J. M. Parpia, Phys. Rev. Lett **74**, 4667 (1995).
16. D. T. Sprague, T. M. Haard, J. B. Kycia, M. R. Rand, Y. Lee, P. J. Hamot, W. P. Halperin, Phys. Rev. Lett. **75**, 661 (1995).
17. G. Ahlers, Rev. Mod. Phys. **52**, 489 (1980).
18. J. Lipa, D. R. Swanson, J. Nissen, T. C. P. Chui, U. E. Israelson, Phys. Rev. Lett. **76**, 944 (1996), and references therein. ■